Advancing the On-Line Enrichment Monitor (OLEM) Capability

James Ely
Rodrigo Guerrero
Benjamin McDonald
Mital Zalavadia

Pacific Northwest National Laboratory
902 Battelle Ave
Richland, WA 99354 USA
E-mail: James.Ely@pnnl.gov

Abstract:

The International Atomic Energy Agency (IAEA) has deployed the On-Line Enrichment Monitor (OLEM) to monitor the enrichment levels of UF_6 gas flowing in header pipes in gaseous centrifuge enrichment plants. A challenge of the measurement is the UF_6 and uranium deposits in the pipe both emit 186 keV gamma-rays from the decay of uranium-235 which is the primary signature for the enrichment measurement. The deposits are therefore an interference in the measurement that is not distinguishable by the gamma-ray signature. For an accurate measurement of the enrichment, the deposit contribution must be estimated and accounted for, typically performed in a post-analysis process. Research is ongoing to explore an approach using the well-known 'dual collimator' approach to measure both the gas and deposits in the same measurement using arrays of cadmium-zinc-telluride (CZT) gamma-ray detectors. This presentation will provide the research status and the modelling and simulation results of this effort. If successful, this approach could provide increased precision and reduced analysis time with a smaller and lighter collection node compared to the current OLEM.

1. Introduction

The International Atomic Energy Agency (IAEA) has developed and deployed an On-Line Enrichment Monitor (OLEM) with the help and development of the US Support Program [1]. The OLEM measures the ^{235}U enrichment of uranium hexafluoride (UF_6) gas in header pipes in enrichment facilities. The OLEM provides advantages over previous and existing systems in that it is unattended, it is mounted on header pipes outside the centrifuge halls, and it does not use radioactive sources.

The OLEM includes a thallium-doped sodium iodide [NaI] gamma-ray detector, a pressure gauge, and a temperature probe, along with the OLEM housing, computer and associated electronics. The NaI detector measures the gamma-ray emissions from a pipe in which UF_6 is flowing. The net counts in a specific region of interest around 186 keV are proportional to the amount of ^{235}U in the field of view of the detector. The pressure and temperature measurements allow determination of the total uranium flowing in the pipe. These three measurements (gamma-ray counts in the region of interest, pressure and temperature) are combined with calibration constants to produce an enrichment value.

The gamma-ray measurement (subtracting background and deposit contributions) is proportional to the ^{235}U density of the UF_6 gas, and the pressure and temperature are proportional to the total uranium density. Dividing one by the other, with the appropriate proportionality constants, results in the ^{235}U enrichment value.

$$E = \frac{Mass\ density\ (^{235}U)}{Mass\ density\ (U_{Total})} = \frac{k(G-B)}{1000 * \frac{4.291P}{T\left[1+\left(-1.3769\times10^{6}\frac{P}{T^3}\right)\right]}}$$

The ^{235}U density is proportional (enrichment constant k) to the net count rate (N) obtained by subtracting the background (B) from the gross (G) count rate. The proportionality or enrichment constant (k) accounts for the pipe geometry and detector efficiency and is constant for a specific pipe and detector. The gross count rate is the response in the gamma-ray detector in a region of interest around 186 keV in the energy spectrum; 186 keV is a dominant gamma-ray emission energy from ^{235}U which forms a peak in the spectrum. The total uranium density (in grams per cubic centimeter or g/cc) is obtained by the UF_6 equation of state using the empirical Weinstock approach [2] along with the pressure (P) and temperature (T) values. Here, pressure is in atmospheres (101.325 kPa or 760 Torr) and the temperature in Kelvin. A factor of 1000 converts the density from g/cc to kg/m^3.

The total background B is a combination of two parts; one background that represents the background underneath the 186 keV peak in the energy distribution spectrum, and another that is within the peak. The background underneath the peak area arises from higher energy gamma-rays that deposit only a fraction of their energy in the detector, either due to external down-scattering or Compton scattering in the detector material itself. The sources can be from higher-energy internal sources (deposits or UF_6 gas) primarily from ^{238}U and its daughters. The background under the peak can also arise from external sources, such as from the natural environment (concrete floors or walls for example) or nearby cylinders or other radioactive sources in the view of the OLEM detector.

The second background contribution, which is in the 186 keV peak itself, is from ^{235}U that is in deposits lining the pipe interior. External ^{235}U contributions to the186 keV peak are insignificant as the detector is shielded. The deposits are uranium solids that form on the pipe walls and arise from several processes. The UF_6 can chemically interact with the wall material and create deposits (passivated surface) or interact with other materials (water vapor for example) and create solid material, typically UO_2F_2, that lines the pipe or can be a radioactive decay ion that gets attached to the wall. In any case, uranium deposits contain ^{235}U which decays and produces a 186 keV gamma-ray which contributes to the ^{235}U peak, the same as the UF_6 gas flowing in the pipe. This deposit background is challenging to determine as it is indistinguishable from the gas contributions in the 186 keV region (see Figure 1).

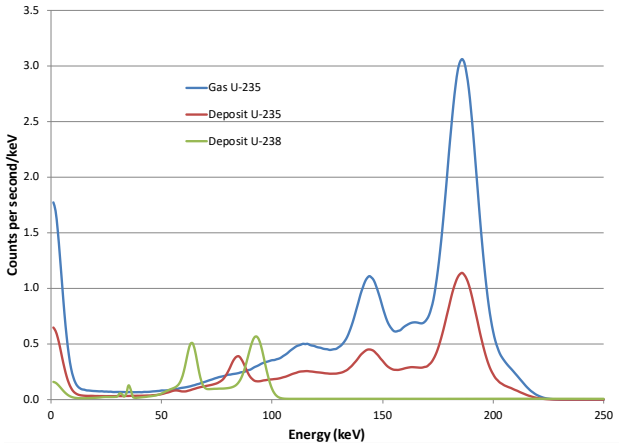

Figure 1. Example simulated energy spectra in a NaI detector of UF_6. The blue line represents the ^{235}U from the gas, the red line is ^{235}U wall deposits, and the green line is ^{238}U from wall deposits.

One of the challenges of the current OLEM is changing deposits. Deposits tend to change over time, and the current OLEM has approaches to estimate the deposits as a function of time. The primary approach is to monitor the gamma-ray count rate as a function of the UF_6 pressure or density, which has a linear proportional relationship. By extrapolating the count rate to zero UF_6 pressure by using the data, one can estimate the deposit contribution. This is shown in Figure 2.

This works well if one has pressure changes (typical in withdrawal header pipes) over a fairly large range to minimize the uncertainty in the extrapolation. However, this requires several post-analysis steps, first to estimate the deposits, the second to calculate the enrichment. And the pressure changes need to be collected over a period of time, when the deposits could be changing as well. A real-time measurement of the deposits would improve the measurement precision and reduce the post-analysis of the data.

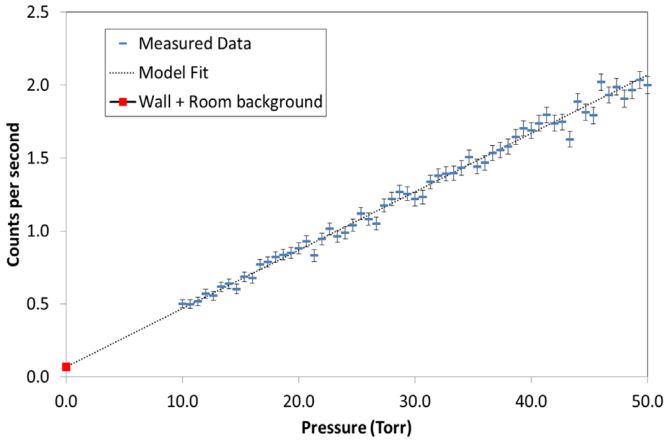

Figure 2. The gamma-ray counts versus pressure for simulated data, illustrating the extrapolation to zero pressure. The y-axis intercept provides the wall deposit (and room background) contribution to the count rate.

There are approaches to measure the deposit contributions in real time using a dual collimator approach [3]. This can be accomplished with either a single detector and a rotating collimator [4] or with multiple detectors [5, 6]. This work explores the possibility of using arrays of cadmium-zinc-telluride (CZT) detectors with two types of collimators to measure gas and deposit contributions in real-time. This would avoid rotating collimators, improve the uncertainty on the enrichment measurement compared to the current system, and reduce the weight and footprint of the system.

2. Dual Collimator Approach

The dual collimator approach makes two measurements using two different geometries; one optimized to measure relatively more of gas compared to the deposits, the other geometry optimized to measure relatively more deposits. By taking two measurement under different geometries, and knowing the detection efficiency for each, the contribution of the gas and deposits can be calculated.

Here we follow the formulism developed by Close and Pratt [3] for the two positions of the collimator, either parallel (∥) or perpendicular to the direction of the gas flow in the pipe (⊦) and the equations therefrom which provide either the gas (G) or the deposits (D) contributions:

$$G = \frac{U\| - \beta U\vdash}{\alpha - \beta}, \quad D = \frac{\alpha U\vdash - U\|}{\alpha - \beta}$$

where ($U\vdash$) is total perpendicular count rate, (U∥) is the total parallel count rate, and α and β are constants and are the efficiency ratios between the perpendicular and parallel collimator geometry.

The uncertainty on the gas count rate in the 186 keV peak can be determined using variance propagation in the first order Taylor expansion, here assuming no covariance:

$$\sigma_G^2 = \left[\frac{U\| - \beta U\vdash}{(\alpha-\beta)^2}\right]^2 \sigma_\alpha^2 + \left[\frac{U\| - \alpha U\vdash}{(\alpha-\beta)^2}\right]^2 \sigma_\beta^2 + \left[\frac{\beta}{(\alpha-\beta)}\right]^2 \sigma_{U\vdash}^2 + \left[\frac{1}{(\alpha-\beta)}\right]^2 \sigma_{U\|}^2$$

3. Modelling and Simulation

To explore the possibility of using detector arrays, models of the pipe, gas, and deposits were developed along with detectors, and simulations performed of the radiation transport into the detectors. This provided estimation of the efficiencies for the gas and deposit contributions and using the formulation described in the previous section, the gas contribution could be estimated. For quantifying the sensitivity of this approach, the uncertainty on the gas contribution, or precision of the measurement, was used as the metric. The accuracy could be used as a metric, but it is governed by a calibration constant (k in the enrichment equation), and any bias is accounted for by infield calibration. Improving the precision or minimizing the uncertainty on the enrichment measurement is the main goal of this exploration, and variations in parameters were simulated to understand the effect on the precision and to optimize the detector and collimators.

The simulation code for radiation transport was Monte Carlo N-Particle (MCNP 6.2) [7]. Models were developed in MCNP of the radioactive source (UF_6 gas and wall deposits), pipe, detectors, collimators, and detector locations. The MCNP simulation results, in terms of energy deposited in the detector as a fraction of the input source activity, were analyzed for the region of interest around the 186 keV peak from ^{235}U emission. These results were used in Microsoft EXCEL to perform scaling variations with respect to the number of detectors, enrichment, pressure, gas-to-deposit ratios, and averaging time, and to calculate the estimated relative uncertainty associated with the gas counts in a system configuration.

The source was modelled in four separate basis models, one for the UF_6 gas, and three for the wall deposits, to allow distinction between the gas and wall deposits, as well as the isotopes. The UF_6 gas is relatively straightforward to model, as it is assumed that there are no ^{238}U decay

daughters present in the freshly enriched gas; therefore, modelled as UF_6 with 5% ^{235}U enrichment. A uniform photon source is added using the ^{235}U major gamma emissions (> 0.5% branching fraction). The ^{238}U daughters are not significant in the UF_6 gas stream.

The wall deposit source was modelled as a thin (10 microns) radioactive layer of UO_2F_2 on the inside of the pipe. For the ^{235}U in the deposits, the gamma-ray emission of the ^{235}U itself is included, with the energies as described above, along with emissions from the daughter ^{231}Th, which has a half-life of 1.063 days. For the ^{238}U chain in the deposits, the main emissions are from the decay daughter ^{234}Th (24.1-day half-life) and ^{234m}Pa (1.17 min half-life).

No other radioactive sources were modelled, such as the room background, since the room background contributions are much smaller that the gas and deposits in the 186 keV region of interest.

Three different pipe models were developed: 2-inch diameter, 4-inch and 6-inch diameter, all Schedule 40. The material was modeled as aluminum and also as stainless steel as a variation. The pipes were modelled as short sections of pipe, each 50 cm long as shown in Figure 3. This length is sufficient to allow for entire coverage of the field of view of the collimated detectors.

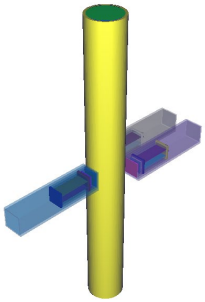

Figure 3. Screen capture of the 3D rendering of the model showing the 2-inch diameter stainless steel pipe and three detector modules.

The detector models were developed using the Ritec CZT model µSpec1500 as the basis detector as shown in Figure 4. The detector material was modelled as a simple cube of CZT of 15 × 15 × 7.5 mm^3. The detector was enclosed in a 3 mm thick tungsten shield of 150 × 33 × 33 mm^3. The detector, as shown in Figure 4, is at the end of the collimator, which was used for simulation where the detector was as close to the pipe as possible. The collimator was sufficiently long to allow for moving the detector within the collimator to provide a standoff distance between the detector and pipe, providing a more collimated, or narrower field of view.

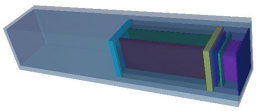

Figure 4. Screen capture of the 3D rendering of the detector model with the detector module inside a tungsten collimator. The detector housing is at the end of the collimator in this image.

The detector array was modelled as three detectors. There was one detector centered on the pipe, and two located near the edge of the pipe (one would have been sufficient, but two were used to understand statistical variation in the MCNP results). Additional detectors were accounted for in the analysis by multiplying either a central detector or an edge detector instead of simulating all possible configurations in MCNP.

For the 2-inch diameter stainless steel pipe, there wasn't sufficient room to put the detectors on a single side of the pipe at the same position along the length, and the edge detectors were

located on the opposite of the pipe for ease of setup and viewing as shown in Figure 5. The detectors on the edge of the pipe are designed to view relatively more of the deposit than the gas in the pipe, and therefore were modelled perpendicular to the pipe.

Once the models were developed, the MCNP simulations were performed. For each photon source (^{235}U, ^{238}U), 2×10^9 particles were simulated and tracked. For each of the three pipe sizes (2, 4, and 6 inch), the four sources were simulated (^{235}U gas, ^{235}U deposit, ^{238}U deposit, ^{234m}Pa beta deposit). The detectors were initially placed at the end of the collimator as close to the pipe as possible. Then the detectors were moved out to stand-off distances of 1, 2, 3, and 4 cm away from the pipe, for a total of 5 different locations. After the initial simulations, the performance of the smallest pipe was fairly poor, with larger relative uncertainties. A new collimator design (see Figure 6) was developed for the smallest pipe that focused on wall of the pipe, rather than the interior, which improved the relative efficiency for the deposits compared to the open collimator with the detector on the side.

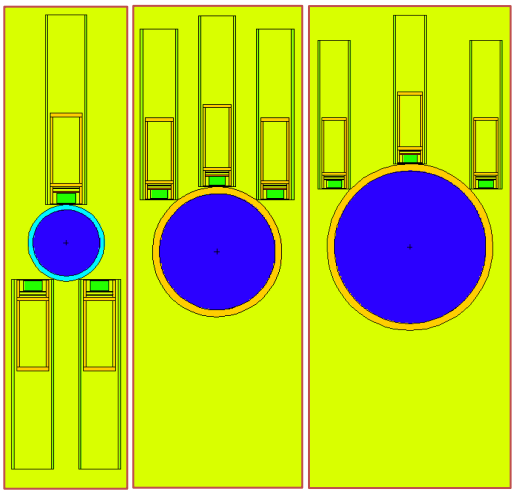

Figure 5. Screen capture of the cutaway rendering of the detector model and pipe for the 2-inch (left), 4-inch (center) and 6-inch diameter pipes (right).

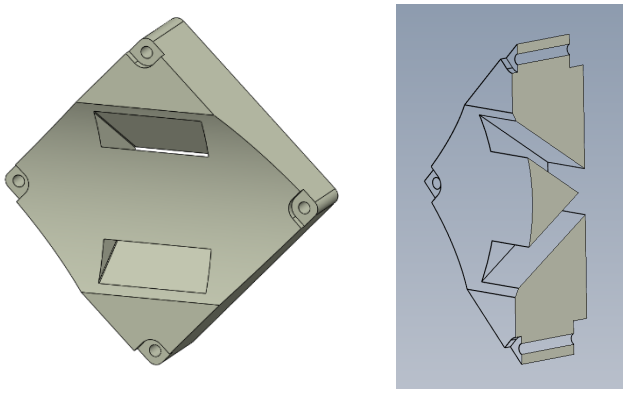

Figure 6. Design of the triangular collimator that shows the opening that focus on the sides of the pipe. Left shows the pipe side of the collimator with the rounded shape to better match the round pipe; right shows a cutaway of the collimator.

The simulation results consisted of the energy deposition in the CZT detectors, and spectra of each of the isotopic contributions were collected. The resulting spectra were post-processed using a set of functions to describe and simulate the detector response [8]. This post-processing step broadens the energy deposition peaks from MCNP and adds a low-energy tailing on the peaks due to incomplete charge collection of CZT. An example of the MCNP simulated results with the energy broadening is shown in Figure 7. The region around the 186 keV peak was

summed and the numbers used with the number of generated particles to determine efficiencies for detection of the various isotopes in the ROI. For this analysis, only the ^{235}U results were used, both the gas and deposits, as the main goal is to determine each contribution.

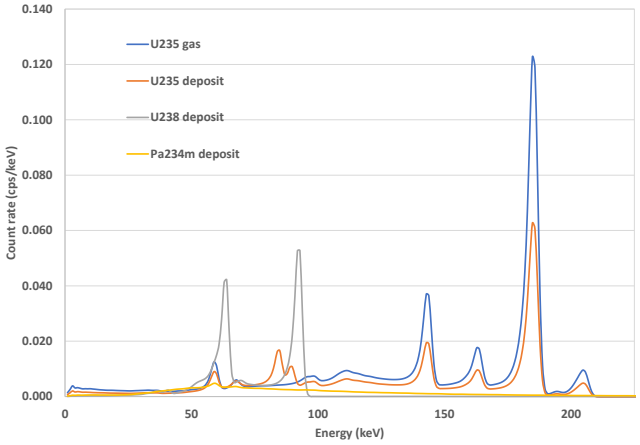

Figure 7. Example of the simulated energy spectra of UF_6 in a CZT detector.

The relative uncertainty in the gas measurement was calculated and explored for the following parameters:

- Three pipe sizes; two, four, and six-inch diameter
- Two pipe materials; aluminum and stainless steel
- Number of detectors, both in the center, and on the side,
- Two collimator and detector positions for the deposits,
- Stand-off distance of the detectors from the pipe,
- Ratio between the contribution from the gas and from the deposits,
- Pressure of the gas,
- Enrichment of the gas and deposits, and
- Averaging time (OLEM measurement time).

As it is difficult to understand the variations of all the parameters at once, a nominal set of parameters was fixed while varying other parameters. This nominal set used representative values and included:

- Enrichment of ^{235}U: 5%
- Pressure: 30 torr
- Averaging time: 4 hours
- Gas-to-deposit ratio: 1:1
- Six total detectors (three pairs).

Each of these parameters were also varied individually to explore their contribution to the overall uncertainty.

4. Modelling and Simulation Results

With all of the parameters and values explored, the results are quite extensive. There are, however, some generalizations that can be made to simplify the understanding and behavior of the results.

For many of the parameters explored including the number of detectors, enrichment, pressure, gas-to-deposit ratios, and averaging times resulted in relative uncertainty values following a square root scaling law. This is to be expected, as the uncertainty in the simulations is dominated by statistics and is the square root of the counts. Increasing the signal by adding detectors, increasing the enrichment, pressure, gas-to-deposits and averaging times, increases the signal linearly, with the uncertainty growing as the square root of the (increased) count rate. For example, the uncertainty as a function of enrichment, shown in Figure 8, illustrates this square root behavior.

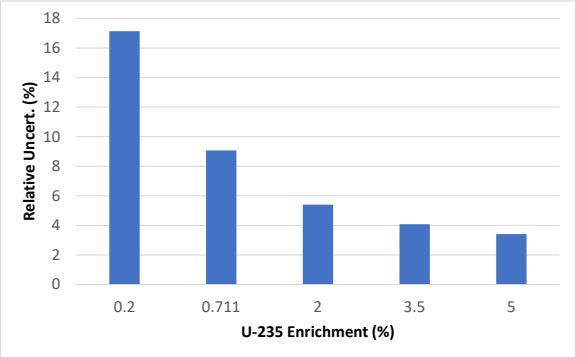

Figure 8. Simulated relative uncertainty of the enrichment measurement as a function of ^{235}U enrichment for the 2-inch diameter pipe with the nominal parameter set.

The larger pipe sizes have larger signals, increasing the count statistics and decreasing the relative uncertainty. The smallest pipe size has the largest uncertainty which increases when switching from aluminum to stainless steel, as the attenuation reduces the signal reaching the detectors. For these reasons, the most challenging case for optimization is the smallest pipe with stainless steel.

The stand-off distance from the pipe for a given set of parameters is the one variable that does not have a linear behavior. As the distance is increased the efficiency drops, but the differentiation power between the gas and deposits increases, and the uncertainty improves (decreases). But at some distance the reduced efficiency drives the uncertainty to larger values. This behavior is shown in Figure 9 for two different square collimator opening sizes, in the case of the same open collimators on all detectors, but offset detectors or the deposits, as was shown in Figure 5. The 1 cm square collimator has an optimum stand-off distance at 1 cm, while the larger 1.5 cm collimator has an optimal stand-off distance of 2 cm.

When moving to the more optimal triangular collimator as described above and shown in Figure 6, the opening slit width of the collimator is another variable that has similar behavior to the stand-off distance. Increasing the collimator opening increases the efficiency, but at some point, the wider opening allows more view of the gas and the discrimination power decreases, resulting in a larger uncertainty on the enrichment. This is shown in Figure 10, where the optimum slit width is 0.45 cm at just under 3.5% relative uncertainty for the nominal parameters set (5% enrichment, 30 torr, 4 hour measurement, gas-to-deposit of 1:1, three pairs of detectors). These modeling and simulation results provide the most optimal parameters for the different cases and values studied, which can be used to design a system.

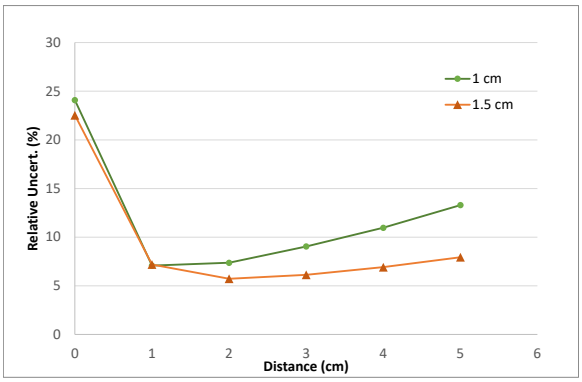

Figure 9. Relative uncertainty as a function of stand-off distance of the detector from the 2-inch pipe for two different collimator openings; 1 cm (green) and 1.5 cm (orange) with the nominal parameter set.

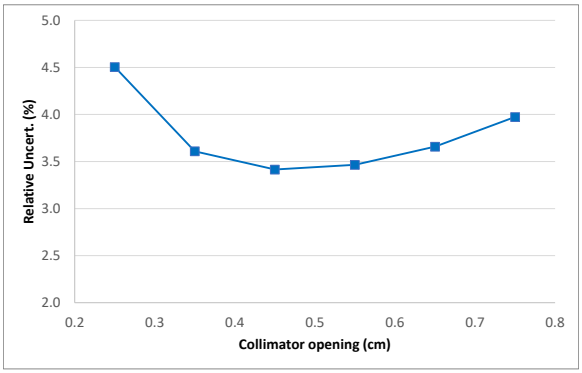

Figure 10. Relative uncertainty as a function of the opening slit width for the collimator on the deposit-viewing detectors for the 2-inch pipe and nominal parameters set.

5. Benchtop Prototype

Based on the promising model and simulation results, a benchtop prototype has been designed and developed. An image of the system in the process of being assembled is shown in Figure 11. This prototype will be useful to validate the simulations, and to demonstrate the capability of this approach. The prototype incorporates three pairs of detectors for a total of six detectors. This provides the ability to validate one, two, or three pairs of detectors in the modeling results, and support extensions to other number of detectors, while minimizing the expense of the prototype.

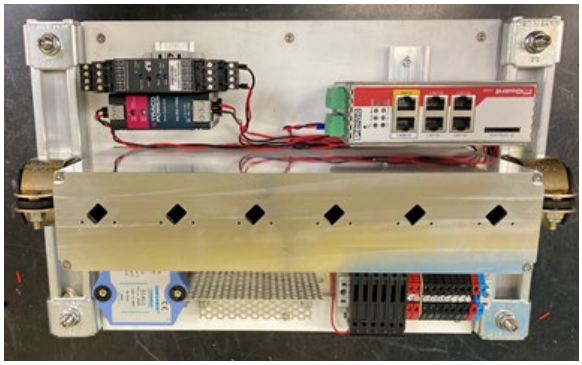

Figure 11. Benchtop prototype in assembly showing the six CZT detector array on top of the pipe. Some additional components will be added in the near future.

The prototype incorporates the triangular type collimator for three of the detectors and open square collimator for the others. The detectors were arrayed in a line along the pipe for a simple layout scheme, and the electronic components arrayed along the side of the detector

housing. Although the design could be made more compact, this benchtop prototype system has about ½ the volume of the current OLEM system, and about ½ the weight.

6. Conclusions

Modeling and simulation of an array of CZT detectors has been performed to explore the possibility of using an array of detectors to measure the gas and deposit contributions in real-time. The results are promising and indicate that the approach will be viable and should reduce the overall uncertainty of the OLEM system in cases where the deposits are changing. This approach will also reduce the post-processing necessary with the current approach for deposit estimation and be viable for installations where the pressure is not changing (e.g., feed header pipes). In addition, the use of an array of CZT detectors should reduce the footprint and weight compared to the current system.

Based on the promising results of the modeling and simulation, a benchtop prototype was designed and is being assembled this year. This will be used to validate the simulation results, and potentially lead to a next generation OLEM system.

5. Acknowledgements

The work presented in this paper was funded by the National Nuclear Security Administration of the Department of Energy, Office of International Nuclear Safeguards.

7. References

[1]https://www.iaea.org/newscenter/news/new-iaea-uranium-enrichment-monitor-verify-iran%E2%80%99s-commitments-under-jcpoa; https://www.energy.gov/nnsa/articles/olem-nnsa-capability-strengthens-global-nuclear-safeguards-mission
[2] DeWitt, R. "Uranium Hexafluoride: A Survey of the Physiochemical Properties," GAT-280, Portsmouth Gaseous Diffusion Plant. 1960.
[3] Close, D. A., J. C. Pratt, and H. F. Atwater, "Development of an Enrichment Measurement Technique and its Application to Enrichment Verification of Gaseous UF6," Nuclear Instruments and Methods A 240, 398. 1985.
[4] Close D. A, J. C. Pratt. "Improvements in Collimator Design for Verification of Uranium Enrichment in Gaseous Centrifuge Header Pipes of Diameter 4.45 cm and 10.16 cm," Nuclear Instruments and Methods in Physics Research A257, 406-411. 1987.
[5] Packer T. W., *et al.*, "Measurement of the Enrichment of Uranium in the Pipework of a Gas Centrifuge Plant," Proc. 6th Annual Symposium on Safeguards and Nuclear Material Management, ESARDA, Venice, Italy, p. 243. 1984.
[6] Favalli, A. *et. al.*, "Multi-detector system approach for unattended uranium enrichment monitoring at gas centrifuge enrichment plants" Nuclear Instruments and Methods in Physics Research A877, 138-142. 2018.
[7] C.J. Werner(editor), "MCNP User's Manual - Code Version 6.2", Los Alamos National Laboratory, report LA-UR-17-29981. 2017.
[8] Mortreau, P., R Berndt., "Characterization of cadmium zinc telluride spectra - application to the analysis of spent fuel spectra", Nuclear Instruments and Methods in Physics Research A458, 183-188. 2001.